JOURNAL OF VIROLOGY, Apr. 1988, p. 1423–1432
0022-538X/88/041423-10$02.00/0

Vol. 62, No. 4

Rapid Induction of B-Cell Lymphomas: Insertional Activation of c-*myb* by Avian Leukosis Virus

MADGE R. KANTER,[1] RALPH E. SMITH,[2] AND WILLIAM S. HAYWARD[1]*

Sloan-Kettering Institute for Cancer Research, 1275 York Avenue, New York, New York 10021,[1] and Department of Microbiology, Colorado State University, Fort Collins, Colorado 80523[2]

Received 13 October 1987/Accepted 30 December 1987

EU-8 is a recombinant avian leukosis virus (ALV) constructed in vitro, which carries long terminal repeats and *gag* and *pol* genes from ring-necked pheasant virus and the *env* gene from UR2AV. Unlike either parent virus, when injected into 10-day-old chicken embryos, EU-8 induces a high incidence of clonally arising B-cell lymphomas within an unusually short latent period, often causing death within 5 to 7 weeks after infection. These tumors differ from the classic lymphoid leukosis induced by ALV in several respects, both biologically and at the molecular level. Most notably, in all of the EU-8-induced tumors examined, the provirus was integrated in the c-*myb* locus, and in no tumors were c-*myc* integrations found. Most of the proviral integrations were downstream of the initiation codon of c-*myb* and thus presumably resulted in some truncation of the c-*myb* gene product, although not to the same extent as has been found in other cases of c-*myb* activation. In addition, several of the proviruses were integrated well upstream of the c-*myb* coding region. This is the first report of ALV interaction with the c-*myb* proto-oncogene and the first report of c-*myb* activation resulting in tumors of lymphoid rather than myeloid origin, suggesting that the target cell specificity of transformation by the *myb* gene is not as restricted as previously believed.

Retroviruses have traditionally been divided into two classes: acute and nonacute. The acute retroviruses carry transforming genes derived from host proto-oncogenes. They cause neoplastic disease with a high incidence, often approaching 100%, and a short latent period of days to weeks. The nonacute retroviruses lack oncogenes and induce neoplasia with a much longer latency, typically 4 to 12 months. Tumors caused by nonacute retroviruses are generally clonal and are thought to result from proviral integration into or adjacent to cellular proto-oncogenes.

Avian leukosis viruses (ALVs), which fall into the latter category of retroviruses, induce a variety of neoplastic diseases in birds, including lymphoma, nephroblastoma, fibrosarcoma, and erythroblastosis (3, 7, 58). The neoplasm most commonly induced by most strains of ALV is a B-cell lymphoma, which originates in the bursa of Fabricius (35, 40). The vast majority of these tumors contain proviral insertions in the c-*myc* locus (16, 23, 38).

ALVs can be classified into subgroups on the basis of host range properties conferred by their envelope glycoprotein (*env*) genes. Ring-necked pheasant virus (RPV), a subgroup-F ALV, has the unusual property of inducing rapidly appearing lung angiosarcomas when injected into 10-day-old chicken embryos (7). The angiosarcomas are not clonal and show no evidence of proto-oncogene activation by proviral insertion (52). In previous studies, the genetic determinant responsible for the induction of lung tumors was localized to the *env* gene of RPV (52). This was done by constructing recombinants between RPV and UR2AV, a subgroup A ALV that does not induce lung angiosarcomas, but induces mainly long-latency *myc*-associated bursal lymphomas typical of most ALVs.

During the course of these experiments, one recombinant, EU-8, which contains the *env* gene of UR2AV and the rest of the viral genome from RPV, was found to induce a high incidence of rapid and lethal lymphomas (52). The progression of the disease induced by EU-8 is distinctly different from that of lymphomas normally induced by ALV; first, the latent period is very short (4 to 8 weeks), and second, the bursa of Fabricius is not extensively involved. Hyperplastic follicles are often seen in the bursa, even at very early times, but they do not develop into nodules or frank tumors. Instead, the organ most extensively involved is the liver.

We report here that the biological differences between EU-8-induced lymphomas and the classical ALV-induced bursal lymphomas reflect basic differences at the molecular level. The genetic components of EU-8 apparently confer upon it the ability to interact not with c-*myc* but with c-*myb*, a proto-oncogene that has not previously been associated with lymphomagenesis. The result is a new and rapid pathway to neoplastic transformation by ALV.

MATERIALS AND METHODS

Virus and cells. The construction (51) and characterization (29, 51) of the EU-8 recombinant virus were described previously. A single virus stock was used for these experiments and propagated in chicken embryo fibroblasts derived from the SC line of White Leghorn chickens (Hyline International, Dallas Center, Iowa). Fibroblasts from the SC line are C/O, gs−, and chf− (1). Virus titer was estimated by reverse transcriptase assays (51), and an estimated 10^5 infectious units of virus was administered to each chicken embryo on day 10 of incubation via a chorioallantoic membrane vein. Chicks were hatched and reared in isolation units. Blood smears (prepared from samples taken from the brachial vein) were obtained twice weekly, and five infected and two uninfected hatchmates were selected for necropsy at weekly intervals. Chickens with distended abdomens were included in the group selected for necropsy (maximum of two per group). Representative tissues were fixed in 10% Formalin, embedded, sectioned, and stained with hematoxylin and eosin according to standard procedures (Colorado HistoPrep, Inc., Fort Collins, Colo.). Bone marrow and liver homogenates were washed in Hanks balanced salt solution

* Corresponding author.

containing 5% calf serum and then cytocentrifuged onto glass slides. Blood smears and organ homogenates were stained with Diff-Quick (Dade Diagnostics, Inc., Aquada, P. R.), and cells were identified by using the morphologic criteria outlined by Lucas and Jamroz (30).

Antibodies and immunofluorescence. Fluorescent-antibody analysis of organ extracts was performed by standard procedures. Briefly, organs were minced, tissue fragments were suspended in ice-cold wash buffer (Hanks balanced salt solution containing 2% calf serum) and homogenized with a loose-fitting homogenizer, and large fragments were removed by sedimentation at 1,000 × *g* for 20 min. Cell suspensions were washed with cold wash buffer, layered onto a solution of Ficoll-Paque (Pharmacia Fine Chemicals, Piscataway, N.J.), and centrifuged at 1,000 × *g* for 15 min. Cells at the interface were harvested, washed, and suspended in cold wash buffer containing 0.01 M NaN_3. Approximately 2×10^6 cells were reacted in suspension with mouse monoclonal antibodies, washed, and centrifuged through a 1-ml cushion of fetal calf serum. The pellet was suspended and stained with fluorescein isothiocyanate-labeled goat anti-mouse immunoglobulin (Sigma Chemical Co., St. Louis, Mo.). The cell suspension was sedimented through a 1-ml cushion of calf serum, washed, and sedimented onto slides. Mouse monoclonal antibodies L-1 and M-4 were used to detect chicken immunoglobulin light and heavy (μ) chains, respectively (9), and the CT-3 monoclonal antibody was used to test for the T3/T4 cell receptor complexes associated with T cells (8).

DNA extraction, restriction endonuclease digestion, and nucleic acid blot hybridization. High-molecular-weight DNA was prepared from frozen tissue as previously described (52). Restriction endonucleases were obtained from New England BioLabs, Inc., Beverly, Mass., or Boehringer Mannheim Biochemicals, Indianapolis, Ind. DNA samples were digested for 3 to 8 h at 37°C with 4 to 6 U of enzyme per μg of DNA.

Digested samples were electrophoresed in 0.7% agarose gels with a buffer containing 0.089 M Tris-borate, 0.089 M boric acid, and 0.002 M EDTA (pH 7.5) and transferred to NYTRAN membrane filters (Schleicher & Schuell, Inc., Keene, N.H.) by the method of Southern (53). After transfer, the filters were baked in an 80°C vacuum oven for 2 h and prehybridized for at least 4 h at 65°C in a solution containing 6× SSC (1× SSC is 0.15 M NaCl plus 0.015 M sodium citrate), 2× Denhardt solution (1× Denhardt solution consists of 0.02% each of Ficoll, polyvinylpyrrolidone, and bovine serum albumin), 0.5 mg of yeast RNA per ml, 50 mM sodium phosphate, and 0.5% sodium dodecyl sulfate. Hybridizations were carried out overnight under the same conditions but with 5% dextran sulfate and 4×10^6 to 8×10^6 Cerenkov cpm of ^{32}P-labeled probe per ml of hybridization solution (3 to 4 ml/100 cm^2). Filters were washed for 10 min at room temperature in 2× SSC, 15 min at room temperature in 1× SSC–0.1% sodium dodecyl sulfate, 30 min at 37°C in 0.2× SSC–0.5% sodium dodecyl sulfate, and 45 min at 65°C in 0.1× SSC–1% sodium dodecyl sulfate.

XAR-5 film (Eastman Kodak Co., Rochester, N.Y.) and intensifying screens were used for autoradiography. To remove the probes, boiling water was poured over filters and allowed to cool to room temperature with occasional agitation. Filters were then exposed to film for 15 to 48 h to ensure that removal of probe was complete; the procedure was repeated if necessary.

RNA extraction, poly(A) selection, glyoxal gel electrophoresis, and Northern (RNA) transfer. Total RNA from tumor samples or normal thymus was isolated by using the guanidinium isothiocyanate method (32), as previously described (52). RNA containing poly(A) was selected by one cycle of chromatography on oligo(dT)-cellulose T-2 (Collaborative Research, Inc., Waltham, Mass.) as described previously (55). Glyoxal gel electrophoresis and Northern transfer were performed as previously described (52), except that 2.5 μg of poly(A)$^+$ RNA was used per lane and RNAs were transferred to NYTRAN filters after electrophoresis. Hybridizations were carried out at 65°C as described for DNA.

Preparation of [^{32}P]DNA probes. High-specific-activity probes (ca. 10^9 Cerenkov cpm/μg of DNA) were prepared by the incorporation of [α-^{32}P]dCTP (3,000 Ci/mmol; New England Nuclear Corp., Boston, Mass.) into double-stranded DNA by random priming (15) with labeling-grade Klenow fragment from Boehringer Mannheim and $p(dN)_6$ primer from Pharmacia.

The following probes were used. The cloned junction fragment, λ8656 fragment, was a 3.8-kilobase (kb) *Eco*RI insert from a λGT10 clone. The *myb* probe was a *Pst*I-*Nde*I fragment of pMK3, a subclone of λ8656 containing an 800-base-pair (bp) *Pst*I-*Eco*RI fragment that includes the first and second v-*myb* homologous exons. U5L was a 315-bp *Eco*RI-*Sac*I insert of the plasmid pU5L (21). U5 was a 540-bp *Pvu*II fragment from pU5, a subclone of pU5L containing a 170-bp *Eco*RI-*Bst*EII fragment. Leader was a 545-bp *Pvu*II fragment from pLead, a subclone of pU5L containing a 175-bp *Bst*EII-*Sac*I fragment. The probe for chicken immunoglobulin light chain was a 2.7-kb *Bam*HI-*Sal*I fragment of the λ(J+C) plasmid kindly provided by Jean-Claude Weill and Claude-Agnes Reynaud (41).

Cloning into λGT10 and screening of library. DNA from tumor 56 was digested to completion with *Eco*RI and size fractionated on sucrose gradients (32). Appropriate fractions were pooled and ligated into *Eco*RI-digested and phosphastase-treated λGT10 arms (Promega Biotech) and packaged with Gigapack packaging extract (Vector Cloning Systems) according to protocols recommended by the manufacturers. The library was screened with the U5L probe as previously described (6). Positive clones were plaque purified, and inserts were subcloned into pUC12 and M13 mp18 and mp19 vectors (33, 61) for sequence analysis by the dideoxy chain termination method (47). Computer analysis of DNA sequence was conducted with the FASTN program of GenBank.

RESULTS

B-cell lymphomas induced rapidly by EU-8. EU-8, when injected into 10-day-old chicken embryos, induces an unusually high incidence of lymphomas within a very short latent period (51). The median age of death is 6 to 7 weeks after infection, but deaths occur as early as 4.5 weeks (3 weeks after hatch).

In a time course study, hyperplastic follicles in the bursa were detected as early as 19 days after infection with EU-8. Despite this, no nodules or tumors were ever detected in the bursa. Microscopic evidence of liver infiltration by lymphoblasts was seen as early as 27 days after infection, and enlarged (three to four times), severely affected livers were detected by 34 days. Among birds that were sacrificed (or died) between 27 and 48 days after infection, 79% (19 of 24) had severe lymphoma. Of birds that survived more than 48 days, only 10% showed signs of lymphoma, presumably because severely involved birds had either died or been selected for sacrifice at earlier times. In birds with heavily

infiltrated livers, it was not uncommon to see increased lymphoblasts in the bone marrow and peripheral blood, although the spillover into the blood seemed to be a late event, seen only in birds with massive liver involvement. Histological sections from a bird with EU-8-induced lymphoma and an uninfected hatchmate are shown in Fig. 1.

Tumor cells identified histologically as lymphoblasts were further characterized by using a DNA probe specific for the chicken immunoglobulin light-chain locus (41). All tumors contained rearrangements of the immunoglobulin light-chain locus and high levels of immunoglobulin mRNAs, suggesting that they were B cells (data not shown). However, because immunoglobulin gene rearrangement is a very early event in chickens (lymphoid cells in the bursa begin to express immunoglobulin M from days 11 to 14 of embryogenesis, the period during which early B cells begin populating the bursa) (22, 25, 31) and because no bursal tumors were observed, we thought it was possible that these cells represented an early lymphoid precursor not yet committed to the B-cell lineage. To address this question, we sought to determine if the cells had undergone immunoglobulin gene conversion events, which are thought to occur in the bursa of Fabricius after VJ rearrangement and which confer upon the developing B cell the sequence diversity required for a full immunologic repertoire (42, 54).

It has been shown that the loss of certain restriction sites in the rearranged immunoglobulin light-chain locus is diagnostic for these conversion events (41, 54). *Sca*I, *Sma*I, and *Kpn*I all cut at sites that are progressively lost during the clonal expansion of B cells in the bursa (54). On the basis of restriction analysis with these enzymes, cells in all of the EU-8 liver tumors had undergone conversion events within the light-chain locus (data not shown). The cells infiltrating the liver and bone marrow reacted with monoclonal antibodies specific for the immunoglobulin light chain and immunoglobulin M heavy chain but did not react with a monoclonal antibody against a chicken T-cell marker (data not shown). Taken together, these data strongly suggest that the tumor cells are fully committed to the B-cell lineage.

Unique U5-positive junction fragments in tumors. The tumors were analyzed for clonality by taking advantage of the *Eco*RI site present in the long terminal repeat (LTR) of EU-8 (Fig. 2A). If the tumor is clonal, hybridization with a probe containing U5 sequences will reveal discrete tumor-specific junction fragments, extending from the *Eco*RI site in the viral 3′ LTR to the first *Eco*RI site in the adjacent cellular DNA (35, 39).

We originally analyzed 12 tumors by this method. An example with two of these tumors is shown in Fig. 2B, with blood cell DNAs as controls for each. The U5L probe hybridized to endogenous proviruses (open arrows) and to the internal 2.4-kb *Eco*RI fragment of EU-8, which were present in all tissues, and to unique junction fragments (3.8 kb in tumor 56 and 3.9 kb in tumor 57; solid arrows), which were present only in DNA from tumor tissues. By using this analysis, we detected unique, tumorspecific, U5-positive junction fragments in a majority of the tumors examined, indicating that these tumors were clonal with respect to proviral integration. Approximately 40% of the tumors had more than one new junction fragment.

Cloning of junction fragment and analysis of integration sites. Unlike previously described ALV-induced lymphomas, none of these tumors contained rearrangements in the c-*myc* locus. We therefore selected six tumors that contained only one new junction fragment for further analysis. Double digestion with *Eco*RI and other enzymes allowed us to construct restriction maps for each junction fragment. For five of the six tumors, the maps were similar, suggesting that most of the tumors contained integrations at a common site. Therefore, we cloned the junction fragment from one of the tumors (tumor 56) into λGT10. A partial restriction map of the clone is shown in Fig. 3A.

Southern analysis of tumor DNAs digested with *Eco*RI and hybridized with a portion of the cloned junction fragment revealed rearrangements in a majority of EU-8-induced tumors (Fig. 3B), indicating that the junction fragment represented a common integration site. The 5.5-kb band present in both normal and tumor tissue represents the germ line configuration of the cloned sequences. We have analyzed a total of 23 liver lymphomas with this clone, and 17 contained rearrangements of this locus that were detectable by *Eco*RI digestion. With one exception, all of the rearranged bands were between 3.8 and 4.5 kb. Three of the tumors had multiple rearrangements of this locus, suggesting that the tumors were oligoclonal in origin. An example of this is tumor 181 (Fig. 3B).

In most cases (75%) the rearranged fragments detected with the cloned junction fragment clearly corresponded to restriction fragments previously detected with the U5 probe (for example, Fig. 2B and 3B, tumors 56 and 57). However, for several tumors, hybridization with the clone allowed the detection of rearrangements that had not been clearly visible as discrete U5-positive junction fragments, either because the band intensity was too low or because they had comigrated with other U5-positive fragments that were not tumor specific.

Rearrangements of this locus were also evident in the DNA of other affected tissues (Fig. 3C). Although blood was initially used as a control tissue, rearrangements of this locus were occasionally detected in blood at low levels (as in Fig. 3C, bird 66). This was consistent with histological observations, which showed elevated lymphoblast levels in the blood of these birds. In general, the intensity of the rearranged band correlated with the proportion of tumor cells seen in the tissue sample. In bird 66, virtually the entire bursa appeared to consist of transformed follicles, hence the strong intensity of the signal from the rearranged band. The fact that only a single rearranged fragment was detected suggests that essentially all of the transformed follicles were derived from the same clonal population. In bird 75, the liver tumor contained two different integrations, both of which were also seen in the bursa and bone marrow. The bursa also contained an additional integration (a minor band at 3.9 kb) not seen in the other tissues.

Integrations located in the c-*myb* locus. To identify portions of the clone that encoded exon information, we digested the DNA clone into several fragments and used each of these as a probe on a Northern blot of normal and tumor RNAs. The 300-bp *Pst*I-*Nde*I fragment (Fig. 3A), which did not contain viral sequences, gave a strong signal on the Northern blot and was therefore selected for nucleotide sequence analysis. By comparing a part of this short sequence to nucleotide sequences in GenBank, we identified it as part of the chicken c-*myb* locus.

Figure 4 is a map of the chicken c-*myb* locus showing the exons of c-*myb* that are also present in the v-*myb* gene of avian myeloblastosis virus (AMV) (18, 27). The 300-bp *Pst*I-*Nde*I fragment contained the entirety of the second v-*myb*-homologous exon plus 65 bp upstream. It is known from analysis of c-*myb* cDNA sequences that there are additional exons that lie 5′ and 3′ of the v-*myb*-homologous exons, but these have not been precisely localized for the

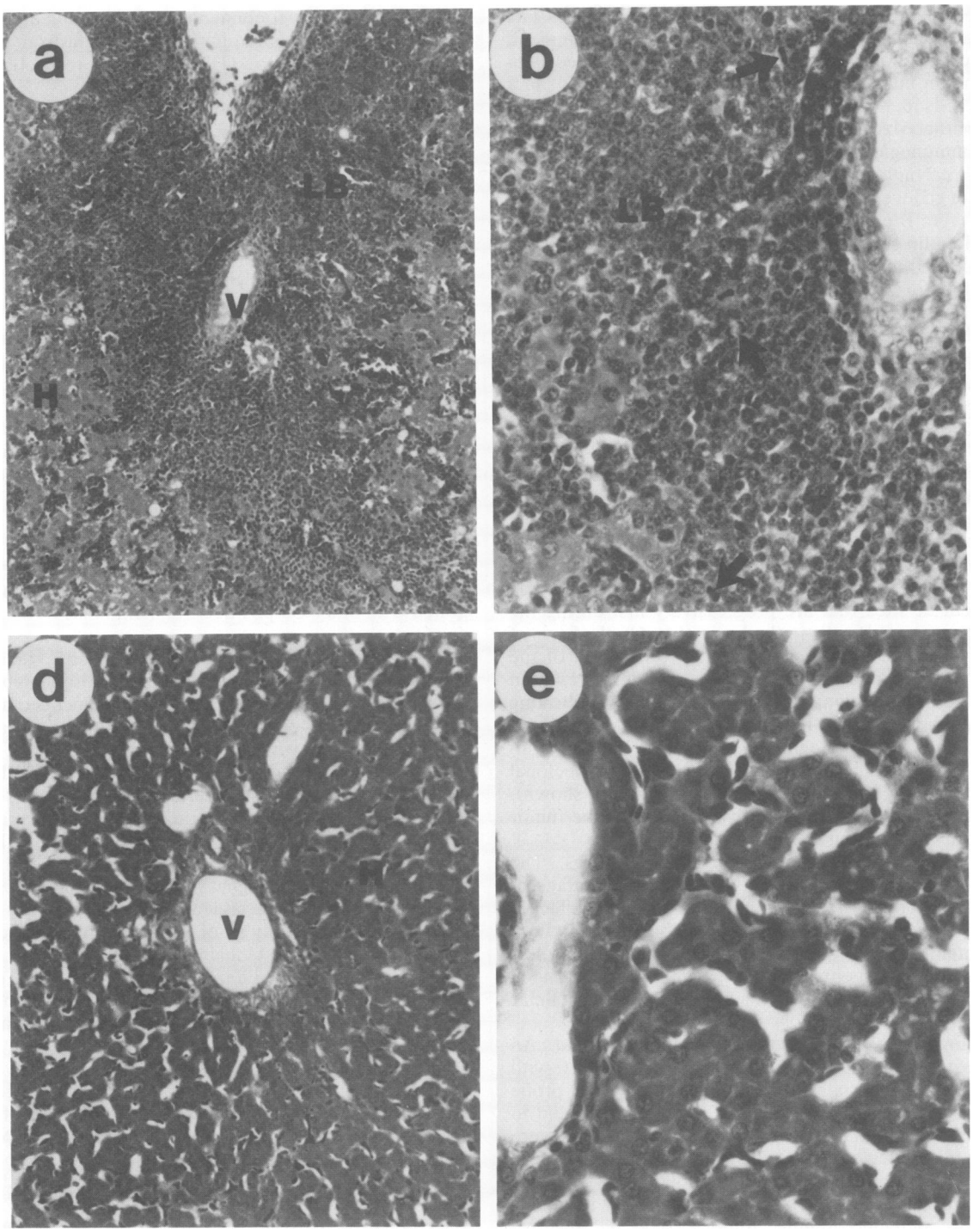

FIG. 1. Tissue sections from a bird with EU-8-induced lymphoma and an uninfected hatchmate. (a to c) Tissue sections from a 24-day-old chicken demonstrating lymphoid leukosis. (d to f) Tissue sections from an uninfected hatchmate. (a and d) Liver sections. Magnification, ×184. (b and e) Liver sections. Magnification, ×552. (c and f) Sections of bursa of Fabricius. Magnification, ×184. (a and b) Lymphoblasts (LB) infiltrating the liver parenchyma and hepatocytes (H) from vascular spaces (V). Mitotic figures (arrows) are frequent. (c) Transformed bursal follicles (single arrows) are disorganized, lacking clear definition of cortex and medulla. Lymphoid infiltrate is present between the follicles (double arrows). (d and e) Vascular space (V) is visible, hepatocytes are arranged in orderly platelike aggregates, and lymphoid tissue and mitotic figures are absent in normal liver. (f) Follicles are arranged in an orderly fashion in normal bursa: each is organized into a clearly defined cortex (c) and medulla (m) that are separated by a single layer of epithelial cells and a basement membrane (arrow). Tissues were stained as described in Materials and Methods.

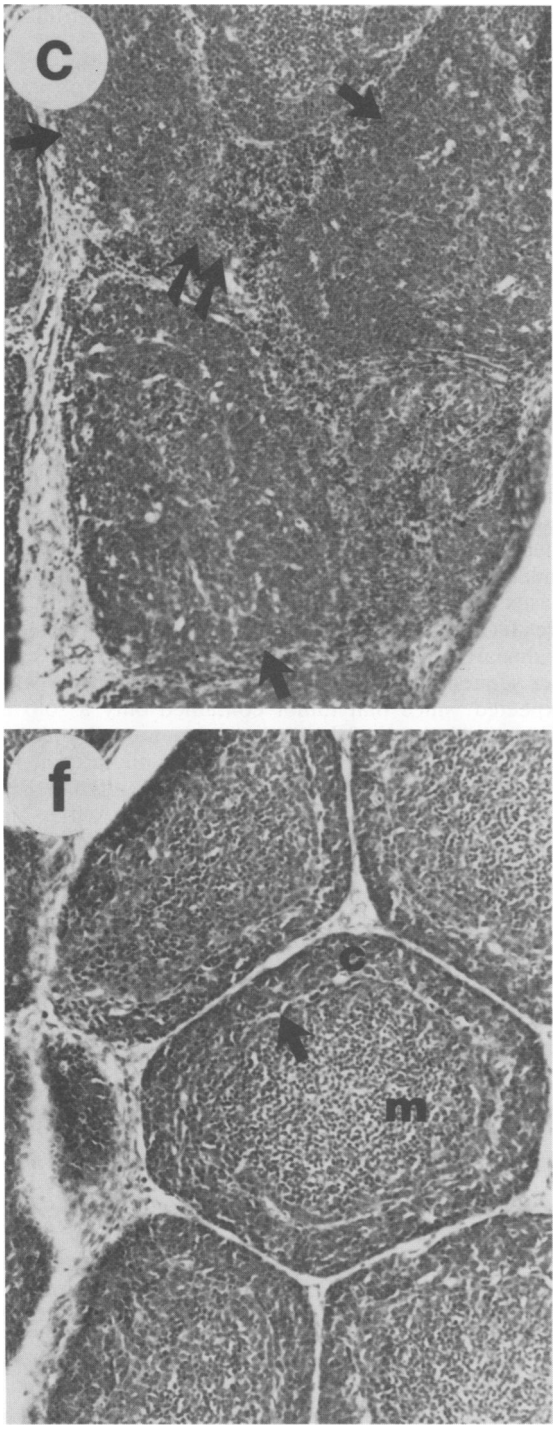

FIG. 1—*Continued*

avian c-*myb* gene (17, 45). Two c-*myb* cDNAs have been sequenced to date, and they differ at their 5′ ends; however, both contain a *Not*I site and are identical downstream from this site (17, 45). Gerondakis and Bishop (17) have presented evidence that c-*myb* translation in B cells is initiated at an AUG just downstream of the *Not*I site. By conducting double digestions of normal chicken DNA with *Not*I plus other restriction endonucleases, we mapped the *Not*I site and other sites (Fig. 4, sites in parentheses) in relation to the v-*myb*-homologous part of the gene.

With this more-extensive mapping information and by using other restriction enzymes, we identified c-*myb* integrations in all of the tumors that did not show rearrangements by *Eco*RI digestion. All of these integrations, detected by *Bam*HI and *Hin*dIII digestions, were located upstream of the *Eco*RI site (Fig. 4). Thus, 100% of the EU-8-induced lymphomas analyzed (23 of 23) had integrations in c-*myb*.

The proviral integrations fell into two classes. Most (75%) of the integrations (those detected by *Eco*RI digestion) were tightly clustered within a 700-bp region approximately 3 kb 5′ of the first v-*myb*-homologous exon (Fig. 4). Since these integrations lay downstream of the *Not*I site, they presumably resulted in synthesis of a truncated c-*myb* mRNA. The remaining six tumors contained integrations upstream of the *Not*I site and thus may not result in truncation. All of the proviruses in the major cluster and two proviruses that were integrated further upstream were in the same transcriptional orientation as the c-*myb* gene. (The transcriptional orientation of the four remaining upstream proviruses has not been

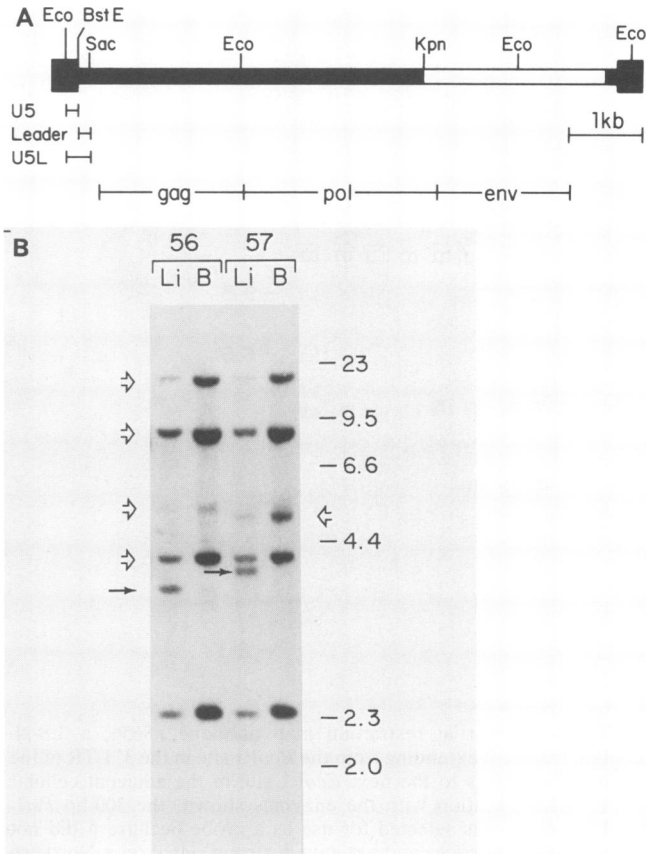

FIG. 2. (A) Restriction map of recombinant EU-8 provirus showing parental origin of sequences and location of viral probes. EU-8 contains LTRs and *gag* and *pol* genes from RPV (■) and the *env* gene from UR2AV (□) (51). The U5 and U5L probes detect a 2.4-kb internal *Eco*RI fragment as well as junction fragments extending from the *Eco*RI site in the 3′ LTR to the next *Eco*RI site in the neighboring host DNA. (B) Restriction analysis of DNA from liver tumors (Li) and control tissue, blood (B), from 2 birds infected with EU-8. *Eco*RI-digested DNAs (8 μg per lane) were blotted and hybridized to a U5L probe. Open arrows indicate fragments derived from endogenous proviruses. Closed arrows indicate tumor-specific junction fragments. The bands at 2.4 kb are the internal viral *Eco*RI fragments detected by the probe, showing that normal, as well as tumor tissues, are infected. Marker sizes are shown in kilobases.

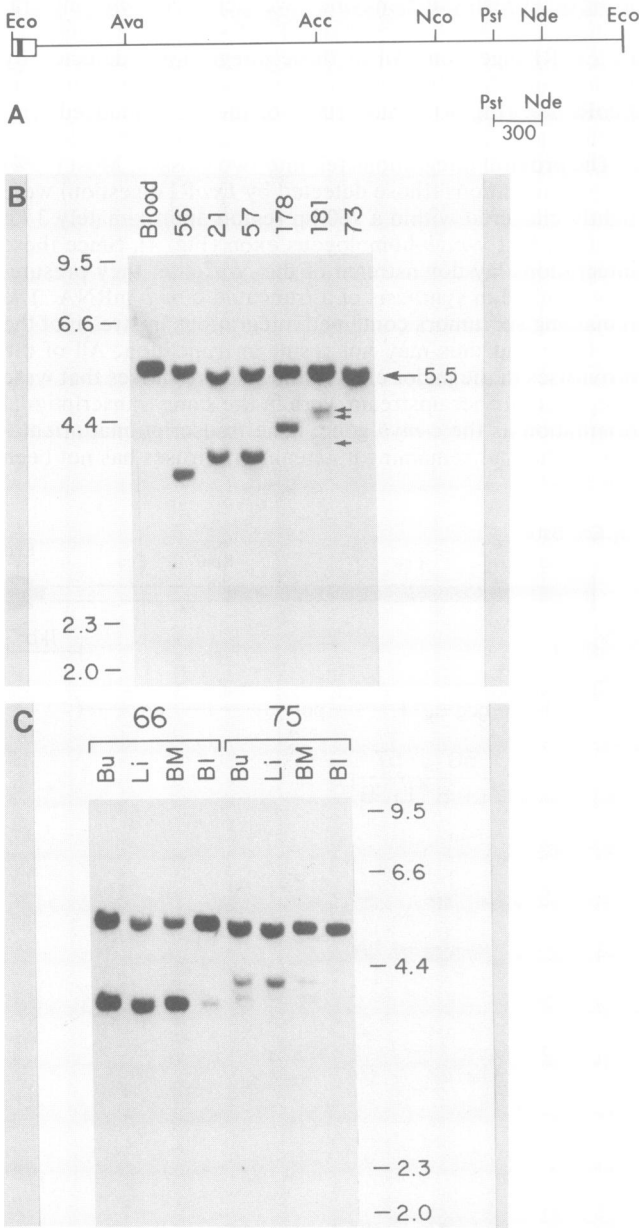

FIG. 3. (A) Partial restriction map of clone λ8656, a 3.8-kb junction fragment extending from the *Eco*RI site in the 3′ LTR of the integrated provirus to the next *Eco*RI site in the adjacent cellular DNA. After digestion with the enzymes shown, the 300-bp *Pst*I-*Nde*I fragment was selected for use as a probe because it did not contain viral sequences and yet gave a strong signal on a Northern blot. (B) Detection of rearrangements in liver tumors. Southern analysis of DNAs from six liver tumors and one control tissue (blood from bird 56) digested with *Eco*RI and hybridized with the 300-bp *Pst*I-*Nde*I fragment of λ8656 is shown. The 5.5-kb band present in all tissues is the normal *Eco*RI fragment detected by the clone. The rearranged bands all lie between 3.8 and 4.5 kb. The tumor from bird 73 did not contain a rearrangement detectable by *Eco*RI digestion. The tumor from bird 181 contained three different rearranged bands (small arrows). (C) Rearrangement of locus in other tissues. Bursa, liver, bone marrow, and blood DNAs were digested with *Eco*RI and hybridized with the same probe used for the analysis shown in panel B.

determined.) We found no evidence for c-*myb*-transducing viruses in these tumors.

Intactness of proviruses. In long-latency lymphomas, integrations into c-*myc* are invariably accompanied by deletions of the provirus, suggesting that, in that system, deletions may have an essential role in oncogenesis (16, 21, 35, 38, 43). In contrast, the majority of the c-*myb*-associated proviruses appeared to be intact, as analyzed by restriction analysis (data not shown), although small deletions or point mutations would not have been detected by this assay. The exception was tumor 56, which contained essentially only a single LTR. The rest of the provirus was deleted.

Northern analysis of tumor RNAs. To determine whether viral LTRs were serving as promoters for *myb* transcription and, if so, which LTR was used, we used a *myb* probe, a probe representing the U5 region of the viral LTR, and a leader probe corresponding to the region of the virus between the 5′ LTR and the 5′ splice site. All transcripts initiating on a viral LTR would hybridize to U5, but only transcripts originating from the 5′ LTR would hybridize to the leader probe (Fig. 2A). Of five tumors tested, all had abundant U5-positive *myb* RNAs (Fig. 5, solid arrows). In all cases except tumor 56, the *myb* RNAs also hybridized to the leader probe; therefore, in these tumors, *myb* transcription appeared to be initiated in the 5′ LTR. The absence of leader sequences on the *myb* message in tumor 56 was not unexpected, since that tumor contained only a solo LTR. The transcripts in all of the tumors were more abundant than those in control tissues, which on our gels migrated at 3.8 kb, and were also altered in size (Fig. 6). (Only thymus RNA is shown as a control, because it demonstrated the highest level of *myb* expression among the normal tissues we examined. Bursa and other hematopoietic tissues have c-*myb* mRNAs of similar size [10, 11, 14, 17, 18, 20, 45].) The

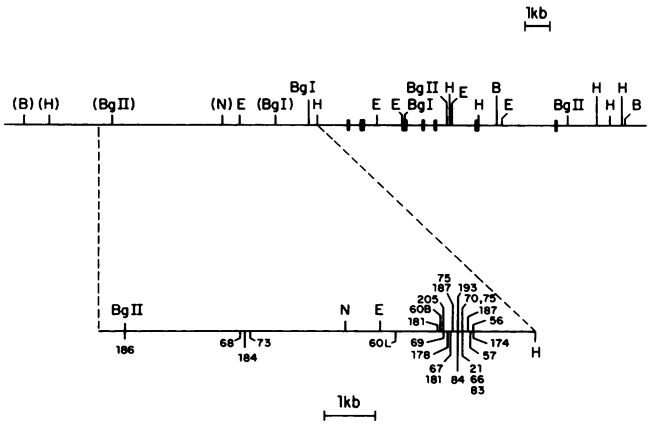

FIG. 4. Partial restriction map of the chicken c-*myb* locus showing EU-8 integration sites. Exons of c-*myb* that are also present in the v-*myb* gene of AMV are indicated by boxes. There are additional exons at the 5′ and 3′ ends that have not been mapped on genomic DNA clones. B, *Bam*HI; Bg I, *Bgl*I; Bg II, *Bgl*II; E, *Eco*RI; H, *Hin*dIII; N, *Not*I. Sites in parentheses were mapped by Southern analysis; locations shown are accurate to ±500 bp. All other sites shown are positioned according to maps of Klempnauer et al. (27) and Gonda et al. (18). (Additional sites for the enzymes shown may exist, particularly in the upstream region which has not yet been cloned.) The major integration cluster spans 700 bp and includes 20 proviral integrations from 17 birds. Six integrations were detected 5′ of the *Not*I site, which maps close to the AUG initiation codon (17); four are shown on the map. The locations of the other two have not yet been precisely determined.

predominant c-*myb* RNA in most tumors was about 4.0 to 4.1 kb, regardless of the site of integration. Since transcriptional initiation within the LTR of proviruses integrated within the major cluster would presumably result in the loss of part of the normal c-*myb* mRNA, the altered transcript must contain additional sequence information, either from the virus or the c-*myb* gene, or both. The exception was tumor 56, which had a transcript somewhat smaller (3.7 kb) than the normal c-*myb* mRNA in thymus.

DISCUSSION

EU-8 is a recombinant ALV that does not carry an oncogene yet induces a high incidence of tumors, with a latent period that is similar to that of some oncogene-positive acute retroviruses (51) (e.g., MC29; see reference 24). The tumors induced by EU-8 differ from previously reported ALV-induced lymphomas, both pathologically and at the molecular level. Most ALV-induced lymphomas originate in the bursa and are believed to progress through specific stages involving multiple transformed follicles at early times, followed by the appearance of one or more discrete nodules, and finally, metastasis to visceral and hematopoietic organs (2, 12, 36). The disease induced by the EU-8 virus resembles classical lymphoid leukosis with respect to the morphology of the tumor cells and the fact that primarily visceral and hematopoietic tissues are involved. Prominant characteristics also include a short latent period and the explosive growth of the transformed cells, often resulting in massive involvement of the liver. In addition, although we have used a strain of chickens which is susceptible to bursal tumors upon infection of the parental viruses RPV and UR2AV, the EU-8 induced disease is characterized by a marked absence of frank bursal tumors (although hyperplastic follicles were observed, often involving substantial portions of the bursa). Taken together, these characteristics appear to distinguish the *myb*-associated lymphomas from the classical *myc*-associated lymphoid leukosis induced by ALV. The EU-8-induced lymphoma is also distinct from nonbursal lymphomas induced by reticuloendotheliosis virus, which appear rapidly but are of T-cell origin and contain integrations in the c-*myc* locus as do the classical ALV-induced B-cell lymphomas (24a, 60).

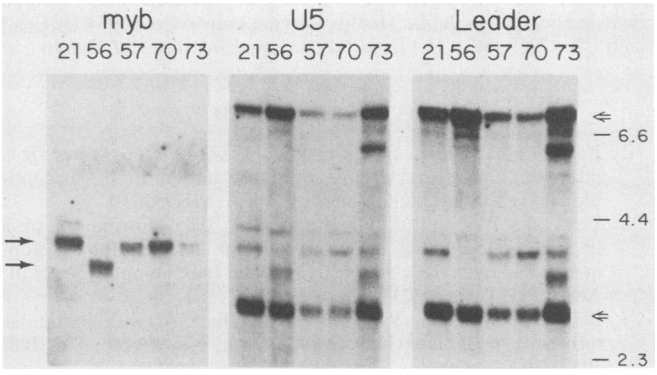

FIG. 5. Northern analysis of poly(A)$^+$ RNA from five liver tumors, four containing integrations within the major cluster and one (tumor 73) with an upstream integration. A single blot was hybridized sequentially with leader, U5, and *myb* probes. Each probe was removed completely before hybridization with the next. Full-length (35S) and subgenomic (21S) viral RNAs are indicated by open arrows. Tumor-specific *myb* mRNAs are designated by closed arrows.

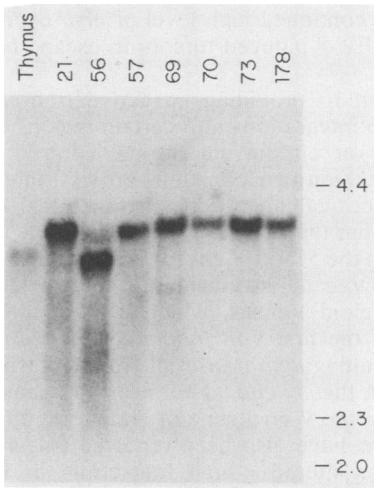

FIG. 6. Comparison of *myb*-specific RNAs in liver tumors and in normal thymus. The same amount of poly(A)$^+$ RNA (2.5 μg) was used for each lane and hybridized with the *Pst*I-*Nde*I probe shown in Fig. 3A.

The origin of the target cells transformed by EU-8 virus is not clear at present, but the presence of surface immunoglobulin M, the absence of a T-cell marker, and the fact that the immunoglobulin genes had undergone rearrangement and conversion strongly suggest that they are B cells.

In 100% of the EU-8-induced tumors analyzed, integration had occurred within the c-*myb* locus, and in no cases were c-*myc* integrations found. Although c-*myb* has previously been implicated in neoplasms of myeloid origin (19, 44, 46, 49, 58), this is the first report of c-*myb* involvement in lymphoid cell transformation. Thus, factors responsive to overproduction or deregulation of c-*myb* and/or alteration of the *myb* gene product must be present in lymphoid cells. This raises questions about why transformation by AMV, both in vivo and in vitro, is specific to myeloid cells. It may be that host factors, specific alterations in the *myb* gene product, and/or genetic determinants of AMV other than v-*myb* are involved in these two systems. It seems likely that other hematopoietic lineages will also respond to an appropriately altered *myb* gene. (In this respect, it is interesting to note that although insertionally activated c-*myc* is associated with B-cell lymphomas, the majority of tumors induced by transduced *myc* genes are of myeloid origin [46, 58].)

The c-*myb* gene is normally expressed at high levels in immature hematopoietic cells, and its expression decreases as the cells mature, suggesting that it plays some role in hematopoiesis (11, 13, 14, 20, 26, 48, 59). Differentiation of myeloid cells is accompanied by a shutoff of *myb* expression (13, 14, 20), and in the murine system, c-*myb* expression progressively decreases as T cells differentiate from immature cortical thymocytes to mature medullary thymocytes and then to resting T cells found in the mesenteric lymph nodes (48). In addition, murine pre-B-cell lymphomas contain 20 to 100 times more c-*myb* mRNA than do the more-mature B-cell lymphomas and plasmacytomas; this fact is thought to reflect the patterns of c-*myb* expression at different stages of normal cell differentiation (4). The reduced transcription in mature cells appears to result from a block-to-chain elongation in the first intron (5). If a shutoff of c-*myb* expression is required for terminal differentiation in B cells,

perhaps the continued high level of *myb* expression allows the cells in EU-8-induced tumors to escape normal growth controls.

In addition to providing an active transcriptional promoter, EU-8 integrations into certain regions of c-*myb* may also disrupt or circumvent normal control regions, thus affecting initiation or elongation. Proviral integration could also cause critical alterations in functional or regulatory domains within the c-*myb* protein. The v-*myb* gene is truncated at both the 5′ and 3′ ends in AMV and E26 (27, 28, 37), and the c-*myb* gene is truncated in murine leukemia virus-induced myeloid tumors, which contain integrations just upstream of the first v-*myb*-homologous exon (19, 34, 49, 50). The resulting *myb* transcripts in the murine tumors are truncated at the 5′ end at or near the same site as the truncation in the v-*myb* gene of AMV; alterations at the 3′ end of c-*myb* have also been reported (44, 49, 56, 57). In contrast, the altered c-*myb* transcripts in EU-8-induced tumors hybridize to cDNA sequences that are 5′ to the first v-*myb*-homologous exon (data not shown). In fact, preliminary data suggest that the majority of the sequences found at the 5′ end of the c-*myb* cDNA, between the *Not*I site and the first v-*myb*-homologous exon, are downstream of the major integration cluster (S. L. Hahn, M. R. Kanter, and W. S. Hayward, unpublished). Therefore, although the *myb* message may be somewhat shortened by these proviral integrations, it is not truncated to the same extent as it is in other systems in which *myb* is activated. In addition, the six upstream integrations lie well upstream of the *Not*I site which, according to one report (17), marks the 5′ end of the *myb* coding sequences. Therefore, in these tumors, *myb* proteins that are initiated at the AUG just downstream of the *Not*I site may not be truncated at all by proviral integrations.

In most murine leukemia virus-induced myeloid tumors, transcription is initiated on the viral 5′ LTR, continues through *gag* to a cryptic splice donor, and then splices directly onto the first v-*myb*-homologous exon, thereby generating transcripts of similar size in all the tumors (44, 49). In all but one of the EU-8 tumors examined, the c-*myb* transcripts were U5- and leader-positive and, thus, were presumably also initiated in the viral 5′ LTR. Since the transcripts are also very similar in size, it is tempting to speculate that they also are generated by the use of a common splice donor and acceptor regardless of the site of integration. If the normal viral 5′ splice site is used, approximately 420 bases of viral sequence would be joined to the c-*myb* sequences. The deletion of most of the provirus in tumor 56 and the resulting absence of leader sequence (approximately 320 bases) would then account for the smaller size of the transcripts in this tumor. Precise determination of transcription patterns, however, awaits the analysis of cDNA clones.

Most ALVs require 4 to 12 months for tumor induction. It has been suggested that this long latency reflects the time needed for subsequent events that are necessary for complete transformation. In fact, recent studies suggest that at least one other locus is insertionally activated in many of the *myc*-associated tumors (B. E. Clurman and W. S. Hayward, unpublished data). One explanation for the short latency of the EU-8 tumors is that a second transforming event is not required for tumor formation in this system, perhaps because events that complement an activated *myb* gene are supplied by the target cell at the time of infection or because the combination of regulatory and structural changes introduced by a single integration event is sufficient to induce a fully malignant state. Alternatively, the target cell population may be expanding so rapidly that the probability of a second event occurring within a short time greatly increases. The proviral deletions associated with lymphomas involving c-*myc* integrations (16, 21, 35, 38, 43) do not appear necessary in these rapid tumors.

The ability of EU-8 to induce rapid lymphomas at high incidence correlates directly with the subgroup-A *env* gene of UR2AV being expressed in the context of RPV-derived LTRs and *gag-pol* genes (51). It is possible that the subgroup-A *env* gene of UR2AV allows the EU-8 virus to infect a target cell not normally accessible to RPV. Once infection has occurred, specific cellular factors may be present to interact with the sequences located in the RPV-derived portion of the genome, resulting in particularly efficient viral gene expression. Nevertheless, the parental UR2AV and several recombinants between RPV and UR2AV do, at low frequency, induce early lymphoid tumors that resemble the EU-8 tumors when injected into 10-day-old chicken embryos (51). Analysis of one of these tumors showed that it also contained a c-*myb* integration. This and other data from our laboratory (Clurman and Hayward, unpublished data) suggest that the ability to insertionally activate the c-*myb* gene is not associated exclusively with the EU-8 virus.

The induction of rapid lymphomas by EU-8 depends on the timing of infection. EU-8 does not cause rapid lymphomas when injected into 1-day-old chicks, presumably because the appropriate target cell or environment is not present at this time or the transformed cells are efficiently cleared by the competent immune system, or both. Thus, both viral and host factors play important roles in determining the disease specificity of EU-8. Under the conditions described here, insertional activation of c-*myb* leads to a new, easily identifiable type of lymphoid leukosis.

ACKNOWLEDGMENTS

We thank Nancy G. Heyman and Jofrid Torgersen for expert technical assistance, Eveyon Maldonado for patient preparation of the manuscript, and Paul O'Donnell, Bruce Clurman, Mitchell Smith, and Maureen Goodenow for helpful comments. We also thank Paul Neiman and Craig Thompson for discussions and suggestions on analysis of chicken immunoglobulin genes and Dan Rosson, Claud-Agnes Reynaud, and Jean-Claude Weill for molecular clones used in these studies.

The generosity of the Morton J. Levy Foundation for financial support to M. R. Kanter is also greatly appreciated. This research was supported by Public Health Service grants CA-35984 (R.E.S.) and CA-43250 (W.S.H.) from the National Institutes of Health.

LITERATURE CITED

1. **Baba, T. W., and E. H. Humphries.** 1984. Avian leukosis virus infection: analysis of viremia and DNA integration in susceptible and resistant chicken lines. J. Virol. **51**:123–130.
2. **Baba, T. W., and E. H. Humphries.** 1985. Formation of a transformed follicle is necessary but not sufficient for development of an avian leukosis virus-induced lymphoma. Proc. Natl. Acad. Sci. USA **82**:213–216.
3. **Beard, J. W.** 1963. Viral tumors of chickens with particular reference to the leukosis complex. Ann. N.Y. Acad. Sci. **108**: 1057–1085.
4. **Bender, T. P., and W. M. Kuehl.** 1986. Structure and expression of c-*myb* proto-oncogene mRNA in murine B cells. Curr. Top. Microbiol. Immunol. **132**:153–158.
5. **Bender, T. P., C. B. Thompson, and W. M. Kuehl.** 1987. Differential expression of c-*myb* mRNA in murine B lymhomas by a block to transcription elongation. Science **237**:1473–1476.
6. **Benton, W. D., and R. W. Davis.** 1977. Screening for gt recombinant clones by hybridization to single plaques *in situ*.

Science 196:180–182.
7. Carter, J. K., S. J. Proctor, and R. E. Smith. 1983. Induction of angiosarcomas by ring-necked pheasant virus. Infect. Immun. 40:310–319.
8. Chen, C. H., L. L. Ager, G. L. Gartland, and M. D. Cooper. 1986. Identification of a T3/TCR complex in chickens. J. Exp. Med. 164:375–380.
9. Chen, C. H., J. E. Leymeyer, and M. D. Cooper. 1982. Evidence for an IgD homologue on chicken lymphocytes. J. Immunol. 129:2580–2585.
10. Chen, J. H. 1980. Expression of endogenous avian myeloblastosis virus information in different chicken cells. J. Virol. 36:162–170.
11. Coll, J., S. Saule, P. Martin, M. D. Raes, C. Lagrou, T. Graf, H. Beug, I. E. Simon, and D. Stehelin. 1983. The cellular oncogenes c-*myc*, c-*myb*, and c-*erb* are transcribed in defined types of avian hematopoietic cells. Exp. Cell. Res. 149:151–162.
12. Cooper, M. D., L. E. Payne, P. B. Dent, B. P. Burmester, and R. A. Good. 1968. Pathogenesis of avian lymphoid leukosis. I. Histogenesis. J. Natl. Cancer Inst. 41:374–389.
13. Craig, R. M., and A. Block. 1982. Early decline in c-*myb* oncogene expression in the differentiation of human myeloblastic leukemia (ML-1) cells induced with 12-0 tetradecanoylphorbol-13 acetate. Cancer Res. 44:442–446.
14. Duprey, S. P., and D. Boettiger. 1985. Developmental regulation of c-*myb* in normal myeloid progenitor cells. Proc. Natl. Acad. Sci. USA 82:6937–6941.
15. Feinberg, A. P., and B. Vegelstein. 1983. A technique for radiolabeling DNA restriction endonuclease fragments to high specific activity. Anal. Biochem. 132:6–13. (Addendum, 137: 266–267, 1984.)
16. Fung, Y.-K., A. M. Fadley, L. B. Crittenden, and H.-J. Kung. 1981. On the mechanism of retrovirus-induced avian lymphoid leukosis: deletion and integration of the proviruses. Proc. Natl. Sci. USA 78:3418–3422.
17. Gerondakis, S., and J. M. Bishop. 1986. Structure of the protein encoded by the chicken proto-oncogene c-*myb*. Mol. Cell. Biol. 6:3677–3684.
18. Gonda, T. J., and J. M. Bishop. 1983. Structure and transcription of the cellular homolog (c-*myb*) of the avian myeloblastosis virus transforming gene (v-*myb*). J. Virol. 46:212–220.
19. Gonda, T. J., S. Cory, P. Sobieszczuk, D. Holtzman, and J. M. Adams. 1987. Generation of altered transcripts by retroviral insertion within the c-*myb* gene in two murine monocytic leukemias. J. Virol. 61:2754–2763.
20. Gonda, T. J., and D. Metcalf. 1984. Expression of *myb*, *myc* and *fos* proto-oncogenes during the differentiation of a murine myeloid leukaemia. Nature (London) 310:249–251.
21. Goodenow, M. M., and W. S. Hayward. 1987. 5′ long terminal repeats of *myc*-associated proviruses appear structurally intact but are functionally impaired in tumors induced by avian leukosis viruses. J. Virol. 61:2489–2498.
22. Grossi, C. E., P. M. Lydyard, and M. D. Cooper. 1976. B-cell ontogeny in the chicken. Ann. Immunol. 127:931–941.
23. Hayward, W. S., B. G. Neel, and S. M. Astrin. 1981. Activation of a cellular *onc* gene by promoter insertion in ALV-induced lymphoid leukosis. Nature (London) 290:475–480.
24. Hayward, W. S., C.-K. Shih, and C. Moscovici. 1983. Induction of bursal lymphoma by myelocytomatosis virus-29 (MC29). UCLA Symp. Mol. Cell. Biol. 5:279–287.
24a. Isfort, R., R. L. Witter, and H.-J. Kung. 1987. c-*myc* activation in an unusual retrovirus-induced avian T-lymphoma resembling Marek's disease: proviral insertion 5′ of exon one enhances the expression of an intron promoter. Oncogene Res. 2:81–94.
25. Kincade, P. W., and M. D. Cooper. 1971. Development and distribution of immunoglobulin-containing cells in the chicken. J. Immunol. 106:371–382.
26. Kirsch, I. R., V. Bertness, J. Silver, and G. F. Hollis. 1986. Regulated expression of the c-*myb* and c-*myc* oncogenes during erythroid differentiation. J. Cell. Biochem. 32:11–21.
27. Klempnauer, K.-H., T. J. Gonda, and J. M. Bishop. 1982. Nucleotide sequence of the retroviral leukemia gene v-*myb* and its cellular progenitor c-*myb*: the architecture of a transduced oncogene. Cell 31:453–463.
28. Klempnauer, K.-H., G. Ramsay, J. M. Bishop, M. G. Moscovici, C. Moscovici, J. P. McGrath, and A. D. Levinson. 1983. The product of the retroviral transforming gene v-*myb* is a truncated version of the protein encoded by the cellular oncogene c-*myb*. Cell 33:345–355.
29. Kogekar, M., T. L. Spurgeon, M. C. Simon, and R. E. Smith. 1987. Proliferative fibromatosis in avian skeletal muscle caused by cloned recombinant avian leukosis virus. Cancer Res. 47: 2083–2091.
30. Lucus, A. M., and C. Jamroz. 1961. Atlas of avian hematology. U.S. Department of Agriculture, Washington, D.C.
31. Lydyard, P. M., C. E. Grossi, and M. D. Cooper. 1976. Ontogeny of B cells in the chicken. I. Sequential development of clonal diversity in the bursa. J. Exp. Med. 144:79–97.
32. Maniatis, T., E. F. Fritsch, and J. Sambrook. 1982. Molecular cloning: a laboratory manual. Cold Spring Harbor Laboratory, Cold Spring Harbor, N.Y.
33. Messing, J., and J. Vieira. 1982. A new pair of M13 vectors for selecting either strand of double-digest restriction fragments. Gene 19:269–276.
34. Mushinski, J. F., M. Potter, S. R. Bauer, and E. P. Reddy. 1983. DNA rearrangement and altered RNA expression of the c-*myb* oncogene in mouse plasmacytoid lymphosarcomas. Science 220:795–798.
35. Neel, B. G., W. S. Hayward, H. L. Robinson, J. Fang, and S. M. Astrin. 1981. Avian leukosis virus-induced tumors have common proviral integration sites and synthesize discrete new RNAs: oncogenesis by promoter insertion. Cell 23:323–334.
36. Neiman, P. E., L. Jordan, R. A. Weiss, and L. N. Payne. 1980. Malignant lymphoma of the bursa of Fabricius and analysis of early transformation. Cold Spring Harbor Symp. Quant. Biol. 7:519–528.
37. Nunn, M., H. Weiher, P. Bullock, and P. Duesberg. 1984. Avian erythroblastosis virus E26: nucleotide sequence of the tripartite oncogene and of the LTR, and analysis of the cellular prototype of the viral *ets* sequence. Virology 139:330–339.
38. Payne, G. S., J. M. Bishop, and H. E. Varmus. 1982. Multiple arrangements of viral DNA and an activated host oncogene (c-*myc*) in bursal lymphomas. Nature (London) 295:209–213.
39. Payne, G. S., S. A. Courteneidge, L. B. Crittenden, A. M. Fadly, J. M. Bishop, and H. E. Varmus. 1981. Analysis of avian leukosis virus DNA and RNA in bursal tumors: viral gene expression is not required for maintenance of tumor state. Cell 23:311–322.
40. Purchase, H. G., W. Okazaki, P. K. Vogt, H. Hanafusa, B. R. Burmester, and L. B. Crittenden. 1977. Oncogenicity of avian leukosis viruses of different subgroups and of mutants of sarcoma viruses. Infect. Immun. 15:423–428.
41. Reynaud, C.-A., V. Anquez, A. Dahan, and J.-C. Weill. 1985. A single rearrangement event generates most of the chicken immunoglobulin light chain diversity. Cell 40:283–291.
42. Reynaud, C.-A., V. Anquez, H. Grimal, and J.-C. Weill. 1987. A hyperconversion mechanism generates the chicken light chain preimmune repertoire. Cell 48:379–388.
43. Robinson, H. L., and G. C. Gagnon. 1986. Patterns of proviral insertion and deletion in avian leukosis virus-induced lymphomas. J. Virol. 57:28–36.
44. Rosson, D., D. Dugan, and E. P. Reddy. 1987. Aberrant splicing events that are induced by proviral integration: implications for *myb* oncogene activation. Proc. Natl. Acad. Sci. USA 84:3171–3175.
45. Rosson, D., and E. P. Reddy. 1986. Nucleotide sequence of chicken c-*myb* complementary DNA and implications for *myb* oncogene activation. Nature (London) 319:604–606.
46. Roussel, M., S. Saule, C. Lagrou, C. Rommens, H. Beug, T. Graf, and D. Stehelin. 1979. Three new types of viral oncogene of cellular origin specific for hematopoietic cell transformation. Nature (London) 281:452–455.
47. Sanger, F., A. R. Coulson, B. G. Barrell, A. J. H. Smith, and B. A. Roe. 1980. Cloning in single-stranded bacteriophage as an aid to rapid DNA sequencing. J. Mol. Biol. 143:161–178.
48. Sheiness, D., and M. Gardinier. 1984. Expression of a proto-

oncogene (proto-*myb*) in hemopoietic tissues of mice. Mol. Cell. Biol. **4**:1206–1212.

49. **Shen-Ong, G. L. C., H. C. Morse III, M. Potter, and J. F. Mushinski.** 1986. Two modes of c-*myb* activation in virus-induced mouse myeloid tumors. Mol. Cell. Biol. **6**:380–392.
50. **Shen-Ong, G. L. C., M. Potter, J. F. Mushinski, S. Lavu, and E. P. Reddy.** 1984. Activation of the c-*myb* locus by viral insertional mutagenesis in plasmacytoid lymphosarcomas. Science **226**:1077–1080.
51. **Simon, M. C., W. S. Neckameyer, W. S. Hayward, and R. E. Smith.** 1987. Genetic determinants of neoplastic diseases induced by a subgroup F avian leukosis virus. J. Virol. **61**:1203–1212.
52. **Simon, M. C., R. E. Smith, and W. S. Hayward.** 1984. Mechanisms of oncogenesis by subgroup F avian leukosis viruses. J. Virol. **52**:1–8.
53. **Southern, E. M.** 1975. Detection of specific sequences among DNA fragments separated by gel electrophoresis. J. Mol. Biol. **98**:503–517.
54. **Thompson, C. B., and P. E. Neiman.** 1987. Somatic diversification of the chicken immunoglobulin light chain gene is limited to the rearranged variable gene segment. Cell **48**:369–378.
55. **Wang, L.-H., P. Duesberg, K. Beemon, and P. K. Vogt.** 1975. Mapping RNase T1-resistant oligonucleotides of avian tumor virus RNAs: sarcoma-specific oligonucleotides are near the poly(A) end and oligonucleotides common to sarcoma and transformation-defective viruses are at the poly(A) end. J. Virol. **16**:1051–1070.
56. **Weinstein, Y., J. L. Cleveland, D. S. Askew, U. R. Rapp, and J. N. Ihle.** 1987. Insertion and truncation of c-*myb* by murine leukemia virus in a myeloid cell line derived from cultures of normal hematopoietic cells. J. Virol. **61**:2339–2343.
57. **Weinstein, Y., J. N. Ihle, S. Lavu, and E. P. Reddy.** 1986. Truncation of the c-*myb* gene by a retroviral integration in an interleukin 3-dependent myeloid leukemia cell line. Proc. Natl. Acad. Sci. USA **83**:5010–5014.
58. **Weiss, R. A., N. M. Teich, H. E. Varmus, and J. M. Coffin (ed.).** 1982. Molecular biology of tumor viruses: RNA tumor viruses. Cold Spring Harbor Laboratory, Cold Spring Harbor, N.Y.
59. **Westin, E. H., R. C. Gallo, S. K. Arya, A. Eva, L. M. Souza, M. A. Baluda, S. A. Aaronson, and F. Wong-Staal.** 1982. Differential expression of the *amv* gene in human hematopoietic cells. Proc. Natl. Acad. Sci. USA **79**:2194–2198.
60. **Witter, R. L., J. M. Sharma, and A. M. Fadly.** 1986. Nonbursal lymphomas induced by nondefective reticuloendotheliosis virus. Avian Pathol. **15**:467–486.
61. **Yanisch-Perron, G., J. Vieira, and J. Messing.** 1985. Improved M13 phage cloning vectors and host strains: nucleotide sequence of the M13 mp18 and pUC19 vectors. Gene **33**:103–119.